



Contents lists available at <http://qu.edu.iq>

Al-Qadisiyah Journal for Engineering Sciences

Journal homepage: <http://qu.edu.iq/journaleng/index.php/IQES>



Improve heat transfer in sudden expansion canal by using obstacle

Mohammed E. Salmsn* and Dhafer A. Hamzah

College of Engineering, Department of Mechanical Engineering at Al-Qadisiyah University, Al-Qadisiyah city, Iraq

ARTICLE INFO

Article history:

Received 07 September 2022

Received in revised form 15 October 2022

Accepted 30 November 2022

Keywords:

Obstacle

Sudden expansion

Streamline

ABSTRACT

The purpose of this investigation is to determine if adding an isolated cylinder to the domain can improve forced convection in the laminar case of the sudden expansion flow in a two-dimensional channel. The range of the Reynolds number (1–200) and the number of prattles 0.71, the impact of different cross-stream locations ($x=10.4, 10.8$ and 11.2) of the circular cylinder on the flow, and thermal properties of the sudden expansion flow have been computationally studied (air). COMSOL Multiphysics is utilized to address the governing continuity, Navier-Stokes, energy equation of energy, and the necessary boundary conditions. Although streamline and isotherm profiles have been used to describe the flow and thermal fields, the temperature dependence of the flow viscosity and thermal conductivity has not been taken into account. The findings presented here demonstrate an improvement in the peak Nusselt value when a circular cylinder is used in comparison to the unobstructed condition.

© 2022 University of Al-Qadisiyah. All rights reserved.

1. Introduction

The process of heat transmission is significantly influenced by flow separation and subsequent reattachment. They can sometimes have negative effects, anything like uneven heat application in thermal devices, but they can also have positive effects, such improving heat transmission at the flow reattachment point. Understanding the fundamental process of temperature difference in flows that are being detached and rejoined is thus crucial for engineering practice. among the most basic geometry where flow detachment and re-attachment occur take place is a backward-facing step. Engineering uses for flow through a backward-facing step include cooling electrical devices, atomic energy devices, Turbine blade cooling channels, Cooling channels for digital devices, and more devices. Numerous research have been done in regard to this geometry, but most of them solely focused on the flow, and it appears that our understanding of heat transmission is still in its infancy. To learn the fundamentals of the

flow split and reconnect events in the laminar flow regime, backward facing step flows under laminar circumstances have been studied both experimentally [7-8] and numerically [9-10]. This study uses an adiabatic circular cylinder in the canal over a wide range of Reynolds numbers when there is a steady two-dimensional fluid motion to investigate the improvement of heat transfer of sudden expansion flows in horizontal canals. However, it is helpful to quickly review the current status of the pertinent literature before beginning a full discussion and presentation of this issue.

2. Problem statement

The physical architecture of a 2-D forced convection research in a sudden expansion channel with a step height (H) and an adiabatic obstacle have

* Corresponding author.

E-mail address: dhafer.hamzah@qu.edu.iq (Mohammed Salmsn)



Nomenclature

C_p specific heat ($J\ kg^{-1}\ K^{-1}$)
 ρ Density ($kg\ m^{-3}$)
 k thermal conductivity ($W\ m^{-1}\ K^{-1}$)

x/s length per inlet height
 H Step height
 Nu_{loc} Local value of Nusselt number
 Nu_{avg} average value of Nusselt number

Pr Number of prantl
 Ra number of Rayleigh
 T Temperature
 U dimensionless velocity of flow in X-direction
 V dimensionless velocity of flow in Y-direction
 Ro dimensionless obstacle radius
 X dimensionless X-coordinates
 Y dimensionless Y-coordinates

Greek symbols

α thermal diffusivity ($m^2\ s^{-1}$)

Θ dimensionless temperature
 \emptyset Angle of obstacle
 μ dynamic viscosity ($kg\ m^{-1}\ s^{-1}$)

Subscripts

avg Value of the Average amount
 o obstacle
 T_c cold temperature
 f fluid (pure water)
 Th hot temperature

Tw Wall temperature

cylindrical shape with a radius (R) at various position dimensions is shown in Figure 1. The basic fluid is air. The backward-facing bottom surface is kept at a high constant temperature (Th), while the extra walls provide thermal insulation. The pace of the step wall varies. The Darcy-Brinkman model is used to simulate channel flow. The expanding area contains an isolated cylinder. The following are the dimensionless parameters that were used in this study: The Reynolds number (Re) 100, 200, and 300, $X_c = 10.4, 10.8, \text{ and } 11.2$, and the Prandtl number was 0.71.

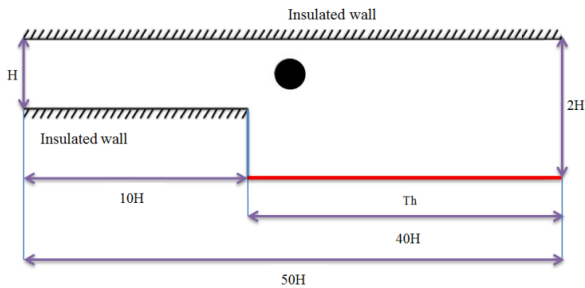


Figure 1 .Boundary conditions and model design for the B.F.S problem with an adiabatic cylindrical obstacle

2.1. Assumption

Avoid hyphenation at the end of a line. Symbols denoting vectors and matrices should be indicated in bold type. Scalar variable names should normally be expressed using italics. Weights and measures should be expressed in SI units. All non-standard abbreviations or symbols must be defined when first mentioned, or a glossary provided. Steady-state.

- Newtonian fluid.
- Flow is incompressible.
- Flow is laminar.
- without energy generation.
- The channel and cylinder walls are considered impermeable.

2.1 The Equation of the conservation

The equation of Continuity:

$$\frac{\partial u}{\partial x} + \frac{\partial v}{\partial y} = 0 \quad (1)$$

The equation of Momentum:

x- Component

$$\frac{\partial u}{\partial x} + \frac{\partial u}{\partial y} = -\frac{1}{\rho} \frac{\partial p}{\partial x} + \frac{\mu}{\rho} \left(\frac{\partial^2 u}{\partial x^2} + \frac{\partial^2 u}{\partial y^2} \right) \quad (2)$$

y- Component

$$\frac{\partial v}{\partial x} + \frac{\partial v}{\partial y} = -\frac{1}{\rho} \frac{\partial p}{\partial y} + \frac{\mu}{\rho} \left(\frac{\partial^2 v}{\partial x^2} + \frac{\partial^2 v}{\partial y^2} \right) \quad (3)$$

Energy equation

$$\frac{\partial T}{\partial x} + \frac{\partial T}{\partial y} = \alpha \left(\frac{\partial^2 T}{\partial x^2} + \frac{\partial^2 T}{\partial y^2} \right) \quad (4)$$

To simplify and minimize the number of variables in equations, especially big equations with many variables, equations are translated into non-dimensional form. Multiple parameters are created by converting variables. The governing equations in the current study were changed by the non-dimensional formula, and the physical characteristics are determined by the flowing non-dimensional parameters[2, 3]:

$$Y = \frac{y}{L}, \quad X = \frac{x}{L}, \quad R = \frac{r}{L}, \quad Re = \frac{\omega r L}{\nu}, \quad u = \frac{uL}{\alpha}, \quad V = \frac{vL}{\alpha}, \quad Pr = \frac{\nu}{\alpha}, \quad \theta = \frac{T - T_c}{T_h - T_c}$$

Non-dimensional governing equations are given by[4, 5].

The equation of Continuity

$$\frac{\partial U}{\partial X} + \frac{\partial V}{\partial Y} = 0 \quad (5)$$

Momentum equation

x- Component

$$U \frac{\partial U}{\partial X} + V \frac{\partial U}{\partial Y} = -\frac{\partial P}{\partial X} + \frac{1}{Re} \left(\frac{\partial^2 U}{\partial X^2} + \frac{\partial^2 U}{\partial Y^2} \right) \quad (6)$$

y- Component

$$U \frac{\partial V}{\partial X} + V \frac{\partial V}{\partial Y} = -\frac{\partial P}{\partial Y} + \frac{1}{Re} \left(\frac{\partial^2 V}{\partial X^2} + \frac{\partial^2 V}{\partial Y^2} \right) \quad (7)$$

Energy equation

$$U \frac{\partial \theta}{\partial X} + V \frac{\partial \theta}{\partial Y} = \frac{1}{RePr} \left(\frac{\partial^2 \theta}{\partial X^2} + \frac{\partial^2 \theta}{\partial Y^2} \right) \quad (8)$$

2.3. Boundary conditions

The non-dimensional boundary conditions are as follows:

On the intake wall.

$$U = 1, V = 0, \text{ and } \theta = 0$$

For the exit:

$$\frac{\partial u}{\partial x} = 0, \frac{\partial v}{\partial x} = 0, \text{ and } \frac{\partial \theta}{\partial x} = 0$$

At the bottom surface after sudden expansion step:

$$T = Th = 1$$

Other horizontal walls is thermal insulated

$$U = 0, V = 0 \text{ and } \frac{\partial \theta}{\partial y} = 0$$

2.2 The Nusselt number

The local and average Nusselt values along the channel's heated bottom surface are calculated as shown in [2, 3, 6]. The influence of various parameters on these coefficients is investigated.

Table 1 . grid size that achieves validation

Predefined mesh	Grid size	Average Nusselt number
Extra Coarse	5855	1.0068
Coarser	9419	1.0098
Coarse	17925	1.0072
Normal	27910	1.0077
Fine	49785	1.0086
Finer	118539	1.0103
Extra Fine	279864	1.0110

Local Nusselt number:

$$Nu(X) = -\frac{\partial \theta}{\partial y} \tag{9}$$

Average Nusselt number on the bottom surface:

$$Nu_{avg} = \frac{1}{L} \int_0^L Nu(X) dX \tag{10}$$

3. Numerical solutions

Because of its successful program for addressing scientific and engineering issues based on partial differential equations, COMSOL Multiphysics CFD Commercial software was employed in the current investigation. COMSOL Multiphysics® version 5.6 software used to resolve the numerical solution. described in this chapter. The P2+P1 Lagrange elements were employed to assure the numerical solution's stability. For finding the local and average Nusselt numbers inside the channel, the governing non-dimensional equations are solved using the finite element method. The CFD solution necessitates the use of a mesh that is appropriate for the computational

domain. To achieve great precision, a significant number of cells is required. As a result, as illustrated in **Figure 2**, the triangular mesh element is used to build the computational domain in a 2-D Cartesian coordinate for a backward-facing expanding channel. It is critical for the PC to tackle a specific problem with minimal processing time and great accuracy. Seven successively revised standardized meshes were examined. The average Nusselt number for all preset grid sizes on the bottom hot wall is evaluated to pick the appropriate grid. The grid-independent test settings are as follows: Re=100, yc=1.5, Xc=10.6 and Pr=0.72. As seen in Error! R eference source not found., those varied from such an Extra coarse grid to an Extra fine. Because the percentage error equals (0.0496%), the Normal mesh was chosen for all situations in this investigation.

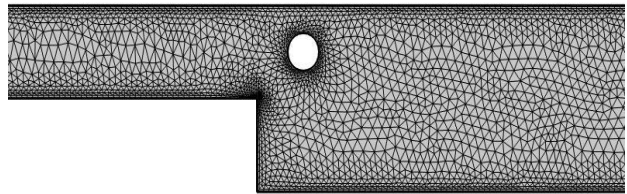


Figure 2 .Shape of element and formation the grid

3.1. Validation

The findings are compared to previous studies to ensure that the COMSOL Multiphysics® software is functional and may be utilized to design and examine the present investigation. Figure 3 illustrates the validation of the local Nusselt number of the present work with Kumar and Dhiman [4]. That investigated the force convection within backward-facing expanding channel with an inner cylindrical obstacle o filled with air at Xc=10.6, Pr=0.72 and yc=1.5.

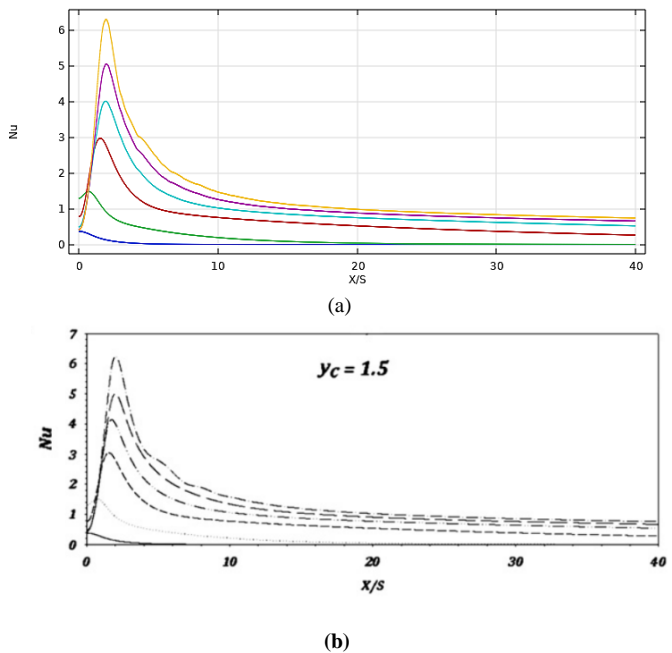


Figure 3. (a) Present work; (b) Kumar and Dhiman [4].

4. Result and discussion

Force convection analysis in a backward facing step with and with insulated cylindrical obstruction. The bottom surface is kept at a high temperature after the stretching step (T_h), while the remaining walls are thermally insulated. For this investigation, the study's parameters were Re , X_o , y_o , and Pr . Parameters values ($Re= 100, 200, \text{ and } 300$), ($X_o= 10.4, 10.8, \text{ and } 11.2$), ($y_o=1.5$), and ($Pr= 0.71$). Figure 4-6 show how the streamlines are affected by the position of a cylinder obstruction for $Re = 100, 200, \text{ and } 300$, respectively. When the barrier is located near the step for the location at $y_o = 1.5S$, the flow coming from the inlet of the canal and hits the obstacle and divided into two amount some pass on obstacle this amount not effect on the separation volume and not effect on heat transfer but anther amount of flow that pass from the way between the obstacle and step height and decrease the separation volume. To ensure a comparative investigation of the impact of the circular cylinder's cross-stream position on flow characteristics, all three cases ($X_o = 10.4, X_o = 10.8, \text{ and } X_o = 11.2$) have been described over the entire Reynolds number range considered. When $X_o= 10.4$ and the cylinder was mounted in the closest position. In this instance, a substantial volume of fluid passes through the space between the cylinder and the step's upper corner. Figures 4(A), 5(A), and 6(A) show the typical fluid flow patterns. for $Re =100, 200, \text{ and } 300$, respectively. In the last two cases ($X_o= 10.8, \text{ and } X_o = 11.2$), it was found that the flow is similar to the first case ($X_o= 10.4$), except that the vortices that formed behind the circular cylinder are of a smaller size.

Flow splits from the rear of the cylinder-shaped obstruction as the Reynolds number rises, creating two slightly downward-directed vortices behind the cylinder. For $100 < Re < 300$, the size of these vortices increases as the Reynolds number increases. It is also observed that as the Reynolds number increases, second separation forms on the upper wall of the step geometry.

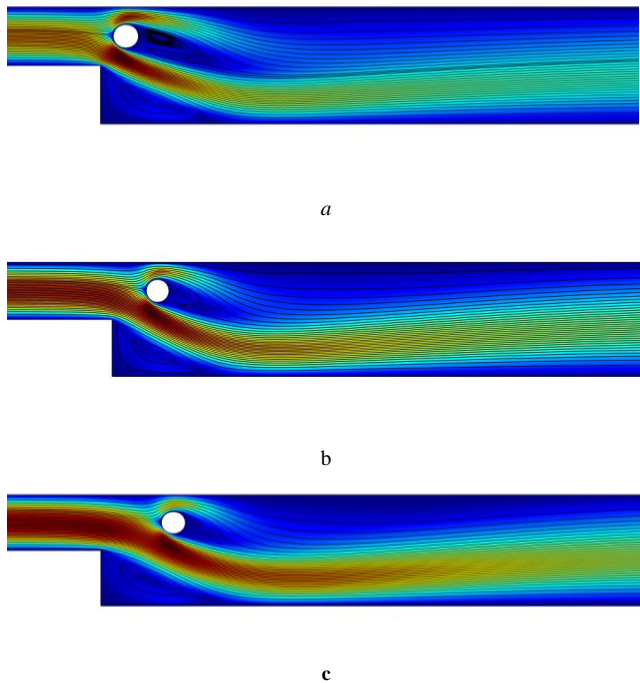


Figure 4. Streamline profiles at $Re =100$: A) $X_o=10.4$, B) $X_o=10.8$, and C) $X_o=11.2$.

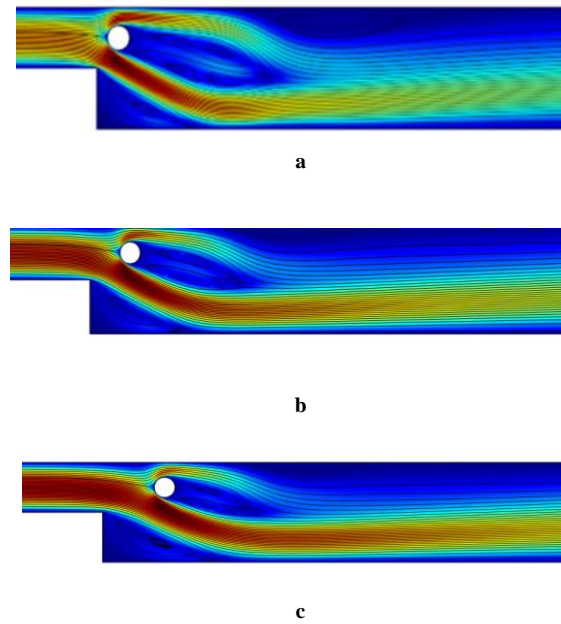


Figure 5. Streamline profiles at $Re =200$: A) $X_o=10.4$, B) $X_o=10.8$, and C) $X_o=11.2$.

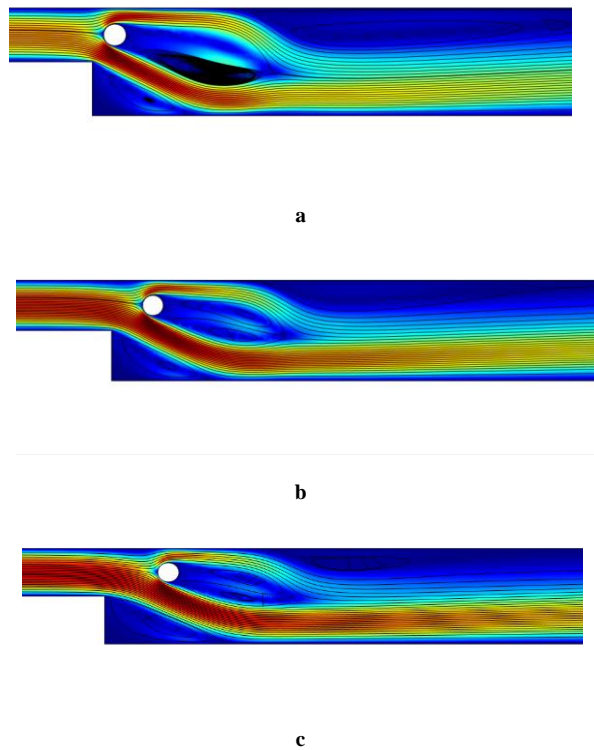


Figure6. Streamline profiles at $Re =300$: A) $X_o=10.4$, B) $X_o=10.8$, and C) $X_o=11.2$.

4.1. Local Nusselt number

Figure 7 depicts the local Nu on the bottom wall for the three different flow configuration positions considered at different Reynolds numbers. According to these figures, with rising Reynolds numbers, the local Nu numbers rise and are at the same distance from step height. Due to the cylindrical obstacle located near the separation area, the streamlines intersect and the separation volume decreases, which leads to an increase in heat exchange between the high-temperature wall and the passing fluid. This figure depicts the variation local Nu for $X_o=10.4S$, and the graph shows that there is a maximum value in Nu. The nature of the local number Nusselt plots in both cases $X_o = 10.8S$, and $X_o=11.2S$ does not differ significantly from flow at $X_o=10.4S$. However, in the first case ($X_o=10.4S$), with highest Reynolds number value ($Re=300$) the highest Nusselt number.

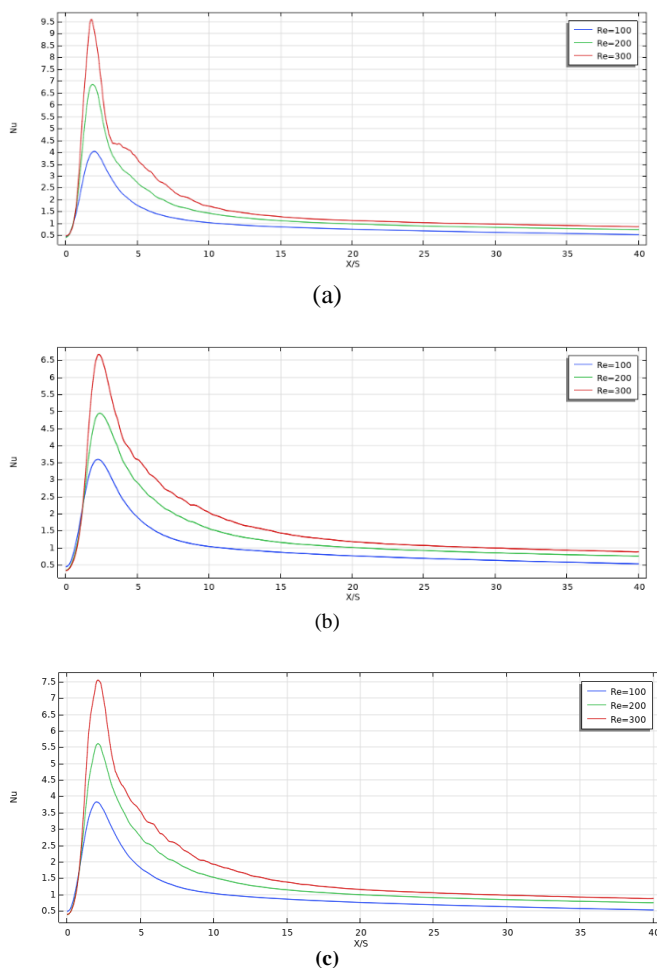


Figure 7. Describes the effect of obstacle location on the Nusselt number at $X_o=10.4$, $X_o=10.8$, and $X_o=11.2$.

5. Conclusion

The adding an isolated cylinder to the domain of the sudden expansion flow in a two-dimensional channel was investigated numerically.

Although streamline of the flow was described as an function of the flow and the temperature, viscosity. The findings presented here demonstrate an improvement in the peak Nusselt value when a circular cylinder is used in comparison to the unobstructed condition.

Authors' contribution

All authors contributed equally to the preparation of this article.

Declaration of competing interest

The authors declare no conflicts of interest.

Funding source

This study didn't receive any specific funds.

REFERENCES

- [1] Togun, H., 2015. Laminar CuO–water nano-fluid flow and heat transfer in a backward-facing step with and without obstacle. *Applied Nanoscience*, 6: p. 1-8.
- [2] Hussain, S.H. and M.S. Rahomey, 2019. Comparison of natural convection around a circular cylinder with different geometries of cylinders inside a square enclosure filled with Ag-nanofluid superposed porous-nanofluid layers. *Journal of Heat Transfer*, 141(2): p. 022501.
- [3] Al-Srattyh, B.M., S. Gao, and S.H. Hussain, 2019. Effects of linearly heated left wall on natural convection within a superposed cavity filled with composite nanofluid-porous layers. *Advanced Powder Technology*, 30(1): p. 55-72.
- [4] Kumar, A. and A.K. Dhiman, 2012, Effect of a circular cylinder on separated forced convection at a backward-facing step. *International Journal of Thermal Sciences*, 52: p. 176-185.
- [5] Anguraj, A. and P. Jothi, 2018, Numerical study of fluid flow and heat transfer in a backward facing step with a rotating cylinder. *Malaya Journal of Matematik*, 06: p. 435-442.
- [6] Boruah, M.P., S. Pati, and P.R. Randive, *Implication of fluid rheology on the hydrothermal and entropy generation characteristics for mixed convective flow in a backward facing step channel with baffle*.
- [7] *International Journal of Heat and Mass Transfer*, 2019. 137: p. 138-160.
- [8] B.F. Armaly, F. Durst, J.C.F. Pereira, B. Schonung, 1983, Experimental and investigation of backward-facing step flow, *J. Fluid Mech.* 127, 473e496.
- [9] M.K. Denham, M.A. Patrick, 1974, Laminar flow over a downstream-facing step in a two-dimensional flow channel, *Trans. Inst. Chem. Eng.* 52, 361e367.
- [10] K. Ichinose, H. Tokunaga, N. Satofuka, 1991, Numerical simulation of two backward-facing step flows, *Trans. JSME B* 57, 3715e3721.
- [11] J.T. Lin, B.F. Armaly, T.S. Chen, 1991, Mixed convection heat-transfer in inclined backward-facing step flows, *Int. J. Heat Mass Transfer* 34,1568e1571.